NASA TECHNICAL NOTE

NASA TN D-5606

c. 1

NASA TN D-5606

DESIGN AND PERFORMANCE OF A DIGITAL ELECTRONIC NORMAL SHOCK POSITION SENSOR FOR MIXED-COMPRESSION INLETS

by Gary L. Cole, George H. Neiner, and Michael J. Crosby

Lewis Research Center
Cleveland, Ohio

NATIONAL AERONAUTICS AND SPACE ADMINISTRATION • WASHINGTON, D. C. • DECEMBER 1969

1. Report No. NASA TN D-5606	2. Government Accession No.	3. Recipient's Catalog No.
4. Title and Subtitle DESIGN AND PERFORMANCE OF A DIGITAL ELECTRONIC NORMAL SHOCK POSITION SENSOR FOR MIXED-COMPRESSION INLETS		5. Report Date December 1969 6. Performing Organization Code
7. Author(s) Gary L. Cole, George H. Neiner, and Michael J. Crosby		8. Performing Organization Report No. E-5223
9. Performing Organization Name and Address Lewis Research Center National Aeronautics and Space Administration Cleveland, Ohio 44135		10. Work Unit No. 720-03 11. Contract or Grant No. 13. Type of Report and Period Covered Technical Note
12. Sponsoring Agency Name and Address National Aeronautics and Space Administration Washington, D.C. 20546		14. Sponsoring Agency Code

15. Supplementary Notes

16. Abstract

The shock sensor described gives a direct indication of a normal shock position by sensing minimums in the cowl-surface static pressure profile. Minimums are determined from outputs of electronic pressure transducers connected to static pressure taps in the inlet throat by means of analog and electronic digital logic elements. Statically the sensor indicates shock position correctly within the spacing of the taps. The sensor response to sinusoidal shock motions of frequencies from 1 to 65 Hz was tested. The results show that the sensor's response is within 10 percent of actual shock amplitude with a phase lag of not more than 18° over the test frequency range.

17. Key Words *(Suggested by Author(s))* Normal shock waves; Supersonic inlets; Sensors; Supersonic test apparatus; Digital systems; Electronic equipment; Shock measuring instruments

18. Distribution Statement Unclassified - unlimited

19. Security Classif. (of this report)	20. Security Classif. (of this page)	21. No. of Pages	22. Price*
Unclassified	Unclassified	29	$3.00

*For sale by the Clearinghouse for Federal Scientific and Technical Information Springfield, Virginia 22151

DESIGN AND PERFORMANCE OF A DIGITAL ELECTRONIC NORMAL SHOCK POSITION SENSOR FOR MIXED-COMPRESSION INLETS

by Gary L. Cole, George H. Neiner, and Michael J. Crosby

Lewis Research Center

SUMMARY

This report describes the development of an electronic digital shock position sensor that was tested in an axisymmetric mixed-compression inlet designed for Mach 2.5. The sensor determines normal shock position by sensing the most upstream minimum in the cowl-surface static pressure profile. Outputs from electronic pressure transducers connected to a series of static pressure taps in the inlet throat are used to determine the static pressure profile. Analog comparators are used to compare the transducer signals from adjacent taps. Each comparator has an ON or OFF output depending on which pressure is larger. The ON-OFF outputs are used to drive electronic digital elements which are arranged to determine the location of the most upstream minimum. The shock sensor produces electrical output voltage levels that, when properly weighted and summed, generate a stepwise continuous signal which is proportional to shock position. Such an output gives a direct measurement of normal shock position, although the resolution is limited to the spacing of the pressure taps.

The sensor was tested both statically and dynamically. Statically, the sensor always indicates shock position correctly. The sensor's response to sinusoidal shock motions at frequencies from 1 to 65 hertz was tested. The sensor is shown to indicate amplitude to within 10 percent of actual shock amplitude over the test frequency range. The sensor's output is also shown to lag actual shock motion by 7° or less out to 35 hertz. The lag increases to 18° at 65 hertz.

No levels are omitted from the sensor's stepwise continuous output signal for frequencies less than 20 hertz. As the frequency increases from 20 to 65 hertz and the shock moves in the downstream direction, levels are sometimes omitted for normal shock positions near the center of shock motion.

The sensor was used in three different ways during wind tunnel programs. The sensor's individual outputs were used to provide a visual indication of normal shock position in the control room. The sensor's stepwise continuous electronic output was used to evaluate normal shock control performance and was used as the feedback variable for a normal shock control system.

INTRODUCTION

To assess the operating condition of a started mixed-compression, supersonic inlet, knowledge of the normal shock location is most desirable. Inlet unstart generally occurs if the normal shock moves upstream of the inlet throat. Thus, shock position is a direct indication of inlet relative stability. Also shock position is an indirect measurement of total pressure recovery.

A signal indicative of shock position is useful for the control of started mixed-compression inlets. This parameter may be displayed to the pilot and utilized as a feedback variable in an automatic inlet control system. On-line measurement and indication of shock position are also useful during research and development testing of inlets.

For downstream disturbances normal shock position can be inferred from an internal inlet pressure measurement downstream of the normal shock. A remote downstream pressure provides a more linear representation of shock position over a larger range of shock positions than does a downstream pressure near the shock. Unfortunately, the gain of a remote pressure to shock position is low, and increased duct dynamics are introduced into the measurement. On the other hand, a pressure near the shock tends to reduce linearity as well as the range of shock positions for which the signal is valid. Furthermore, a pressure downstream of the shock does not necessarily provide a signal which is proportional to shock position when shock motion results from upstream disturbances. The downstream pressure signal is thus a satisfactory feedback variable (representative of normal shock position) only when shock motion is caused by disturbances originating downstream of the shock. In an attempt to measure normal shock position directly, a scheme was developed which determined normal shock position by comparison of a series of cowl-surface static pressures. Both electronic and flueric implementations of the sensing scheme were made. This report describes the development of the electronic sensor. The logic used to determine shock position is a modified version of that developed for the flueric shock sensor which is reported in reference 1.

Static and dynamic tests of the shock sensor were conducted in the Lewis 10- by 10-Foot Supersonic Wind Tunnel on an axisymmetric mixed-compression inlet. Results of the tests are presented and the performance of the sensor is analyzed. The sensor's output as a measure of shock motion is then compared with shock motion as indicated by a single static pressure downstream of the shock. Use of the sensor's output as a diagnostic device as well as a visual aid for determining shock position is discussed.

SYMBOLS

A, B, C, D, E, F, G, H	static pressure taps on inlet cowl surface (also refers to pressures measured at those taps)
AND	logical AND function (has the value true only if all inputs have the value true)
e_b	pressure bias voltage, V
OR	logical OR function (has the value true if any input has the value true)
P	static pressure, N/cm^2
S_{xy}	outputs of electronic shock sensor - indicates existence of a normal shock between x and y or that an output exists for a shock position further upstream
t	time, sec
x	normal shock position, cm
ΔA_{by}	zero to peak amplitude of sinusoidal bypass door disturbance, m^2
ΔE	zero to peak command voltage to bypass door servos, V
Δx	zero to peak amplitude of normal shock motion, cm
φ	phase angle, deg or rad
ω	frequency, radians/sec
Subscripts:	
A, B, C, D, E, F, G, H	refers to pressure taps, A to H, respectively
a	refers to actual normal shock motion measured by tap crossings
ds-H	normal shock located downstream of tap H
i	refers to indicated shock motion measured by frequency response analyzer analysis of the shock sensor output
OL	refers to value of quantity obtained without control (open loop)
s	refers to normal shock motion measured by fitting shock sensor output with sine wave by method of least squares
us-B	normal shock located upstream of tap B
56	throat exit location (see fig. 7)

DESIGN APPROACH

Criteria for Establishing Normal Shock Position

In an ideal supersonic inlet, the supersonic static pressure profile downstream of the throat would show static pressure decreasing in the downstream direction. The presence of the normal shock would be indicated by a strong positive pressure gradient. Thus, one criterion for establishing the location of a normal shock in an ideal inlet would be to detect the minimum point in the static pressure profile. Since it is not possible to measure a continuous static pressure distribution, the pressure profile could be determined by a series of closely spaced static pressure taps. A criterion for establishing normal shock position would then be to find the minimum pressure by comparing three consecutive pressure taps. The shock would be located between the tap showing the minimum pressure and the adjacent downstream tap. A shock location downstream of the last tap would be indicated when the pressure at the last tap was less than the pressure at the adjacent upstream tap. Shock position error could then be no greater than the tap spacing, except when the shock is not located within the region of the taps.

Unfortunately, inlets having a high degree of internal contraction and bleed flows in the region of the inlet throat exhibit irregular, nonideal pressure profiles. The inlet in which the shock sensor was tested exhibited such irregular profiles. Figure 1 shows cowl-surface static pressure profiles in the vicinity of the normal shock for various shock locations. The profiles were measured by means of electronic pressure transducers connected to the eight static pressure taps located in the inlet throat (tap A to H). The dashed line in figure 1 is the supersonic pressure profile in the inlet throat which occurs when the shock is downstream of H. Ideally, that curve should show pressure continuously decreasing in the downstream direction. This is obviously not the case, and it is suspected that the irregular supersonic pressure profiles are primarily due to the porous bleed regions on the inlet cowl surface. The locations of the bleed regions are indicated in figure 1. As the normal shock advances in the upstream direction (from H to A) the pressure rise associated with the shock begins to appear. It is noted that irregularities also occur in the pressure profiles for shock positions upstream of tap H. If the criterion for establishing shock position from minimums in the pressure profile is applied to the profiles of figure 1, it can be seen that more than one shock would be indicated in some cases. For example, the pressure profile denoted by the symbol □ would indicate that a normal shock exists between taps B and C, between taps E and F, and downstream of tap H. One can visually establish the approximate normal shock position to be between taps B and C by the strong positive pressure gradient. The other two indicated shock positions can be attributed to the phenomenon which produced irregularities in the supersonic profile. Thus, the simple criterion of detecting

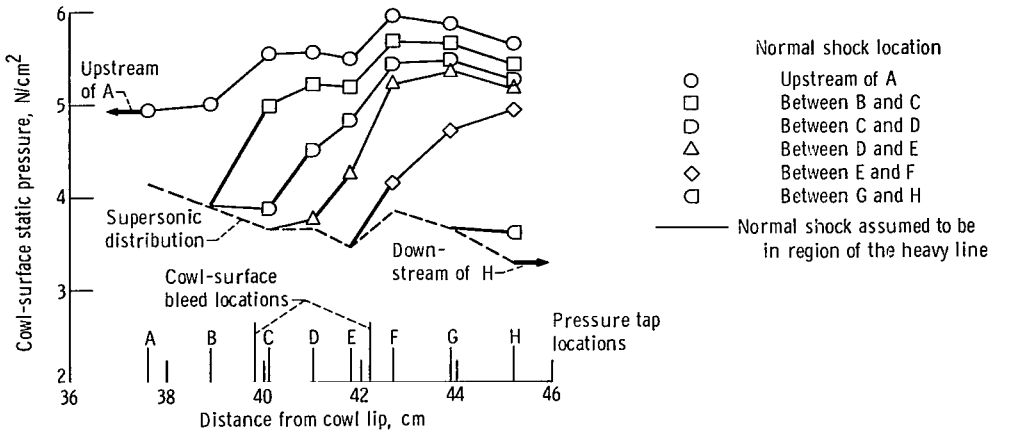

Figure 1. - Typical inlet cowl-surface static-pressure distributions for various shock positions. Free-stream Mach number, 2.50; angle of attack, zero.

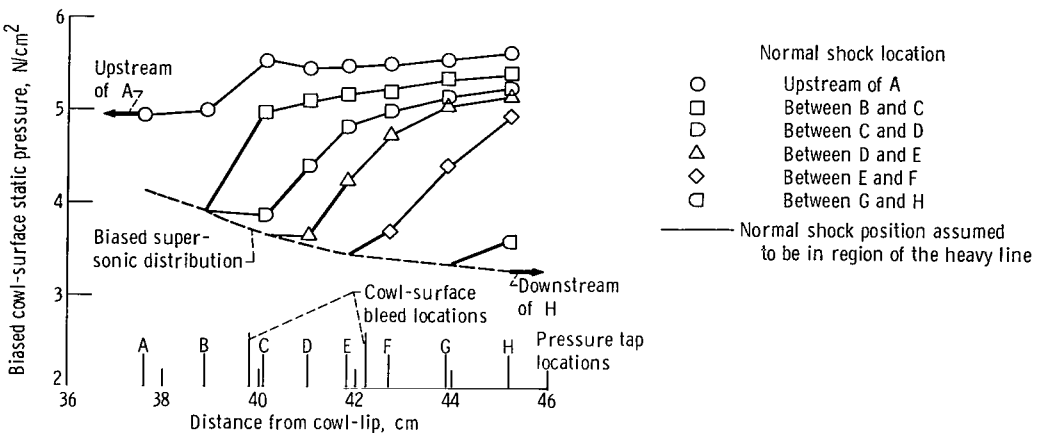

Figure 2. - Effect on pressure profiles of figure 1 due to subtracting biases at taps D, F, and G of 0.1, 0.45, and 0.3 newtons per square centimeter, respectively. (Note that assumed shock positions are not changed from fig. 1)

a minimum in the static pressure profile is not sufficient for establishing normal shock position in the real inlet.

The minimums which give false indications of shock position could be eliminated by biasing the individual pressures measured at the taps. Since the pressures were converted to electrical signals by the transducers, the biasing could be done electronically. An example of how the pressure profiles of figure 1 could be changed with biasing is shown in figure 2. These profiles came about by arbitrarily subtracting pressure biases

at taps D, F, and G of 0.10, 0.45, and 0.3 newtons per square centimeter, respectively. The biased supersonic pressure distribution is ideal in the sense that the pressure continuously decreases in the downstream direction. In addition, only one false minimum is exhibited by the biased profiles. That occurs in the profile denoted by the symbol ◯ where a false shock position is indicated between taps D and E, due to the minimum at tap D. Therefore normal shock position is defined as being at the most forward location of indicated pressure profile minimums where the pressures being measured would be biased to give profiles similar to those of figure 2.

A logic circuit for establishing normal shock position according to the most upstream minimum criterion is shown schematically in figure 3. The pressures at each pair of adjacent taps are first compared to determine which is larger. The comparator outputs indicate which inequality is true as shown by a heavy line in the figure. The appropriate pair of comparator outputs for three successive taps are then passed through an AND gate. The AND gate will have an output only if both inequalities are true. Thus, if an AND gate has an output it means that a minimum occurs at the center tap. This indicates a shock position between the center tap and the adjacent downstream tap. For example, a minimum can occur at tap C only if the inequalities $B > C$ and $C < D$ are true. The output units (logical OR elements) are connected in such a way that the actual shock position output and all downstream outputs are turned on. In this way, all false indications of a shock downstream of the actual shock position are ignored. The outputs shown in figure 3 are for the case when the shock is located between taps C and D and no false minimums occur. If a false minimum did occur downstream of the shock, it would be of no consequence because all downstream outputs are already turned on. The

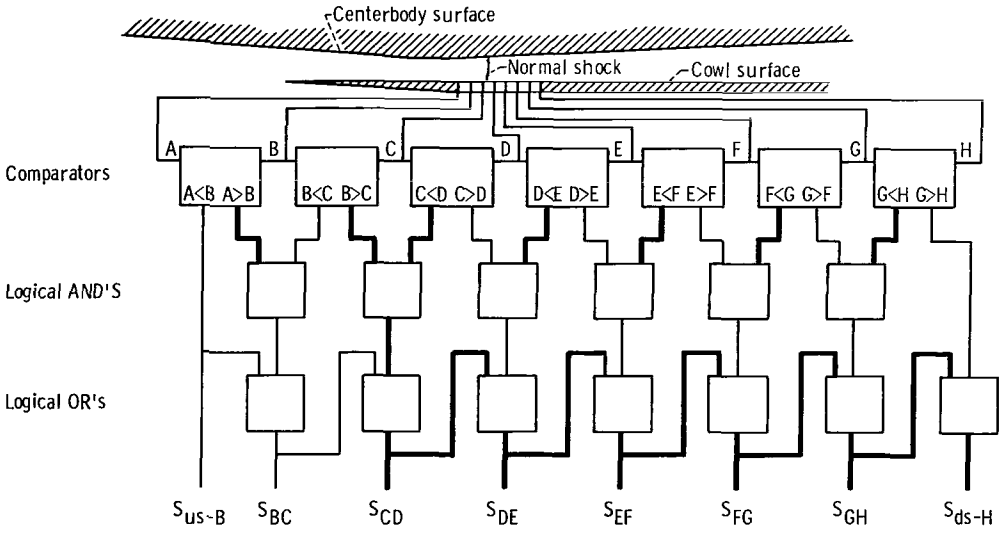

Figure 3. - Schematic representation of logic used to establish shock position. Case shown is for shock location between taps C and D; heavy lines indicate ON or true outputs.

shock position criterion assumes that no false upstream minimums will occur since the pressures can be biased to eliminate them.

Electronic Circuit Design

The shock sensor logic shown schematically in figure 3 can be implemented electronically by means of the circuit which is shown schematically in figure 4. The circuit of figure 4 follows directly from figure 3; and, although it is not identical to the circuit that was tested, it will be discussed first.

Outputs of the transducers connected to the throat static pressure taps are trunked to analog comparators where appropriate biases are added. One inequality of each complementary pair (e.g., either $A < B$ or $A > B$) is first established by a comparator. The comparators are composed of analog components connected in such a manner that an output exists only when the inequality indicated is true. The complementary inequalities are obtained by passing the ON-OFF outputs of the comparators through digital logical inverters. Thus, for the case when $A > B$ is true, the comparator would have an ON output and the logical inverter which establishes the inequality $B > A$ would have an OFF output. ON or true outputs are indicated in figure 4 by the heavy lines. The

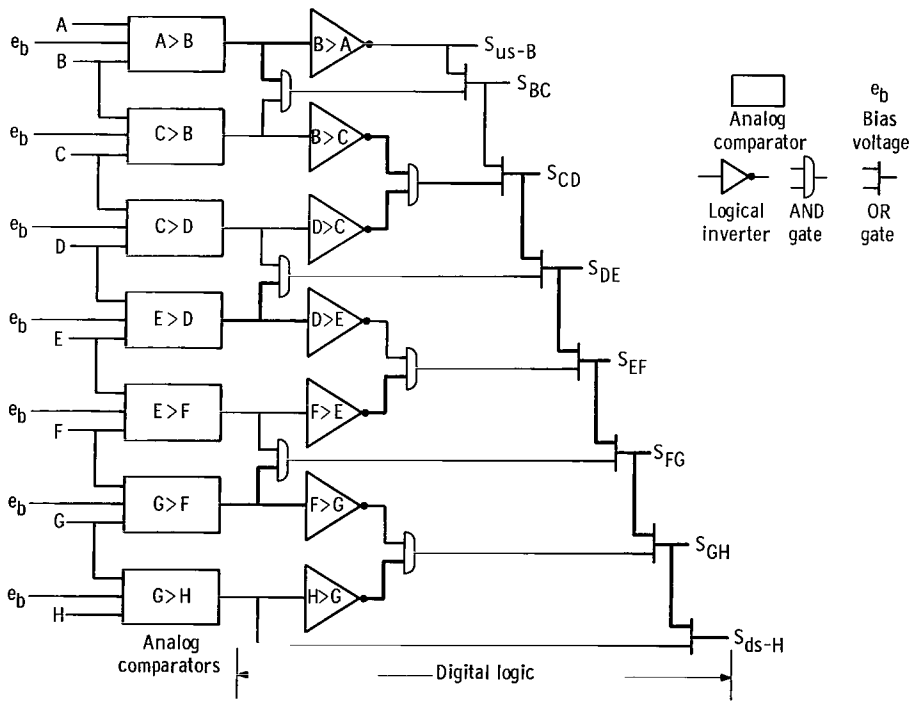

Figure 4. - Electronic implementation of shock sensor logic shown in figure 3. Case shown is for shock between taps C and D.

specific case of the shock existing between taps C and D is illustrated. Minimums in the pressure profile are detected by means of the AND gates. An AND gate has an output only when both inputs are true. The outputs of the AND gates are connected to the OR gates which will have outputs if either input is true. It is noted that, for the case shown, the S_{CD} output triggers all the outputs downstream of S_{CD}. Detection of a minimum downstream of the normal shock would be of no consequence since the downstream S outputs are already turned on. As was mentioned earlier, the pressure signals are biased to eliminate false indications of a shock position upstream of the actual shock position. Since the distances between the taps are not equal, each S output is made proportional to the distance between the taps. The S outputs are then summed by means of analog summing amplifiers which generate an electronic stepwise continuous signal which is proportional to shock position. When the shock is downstream of H only the S_{ds-H} output is on, thus giving the minimum value of the step signal. As the shock advances in the upstream direction, additional S outputs are turned on, thus being added to the signal.

The shock sensor circuit, for which test results will be shown later, is shown schematically in figure 5. The circuits of figures 4 and 5 have equivalent logic and they would have produced the same results. The circuit of figure 5 was used because it was a simpler circuit, requiring fewer components, than the circuit shown in figure 4.

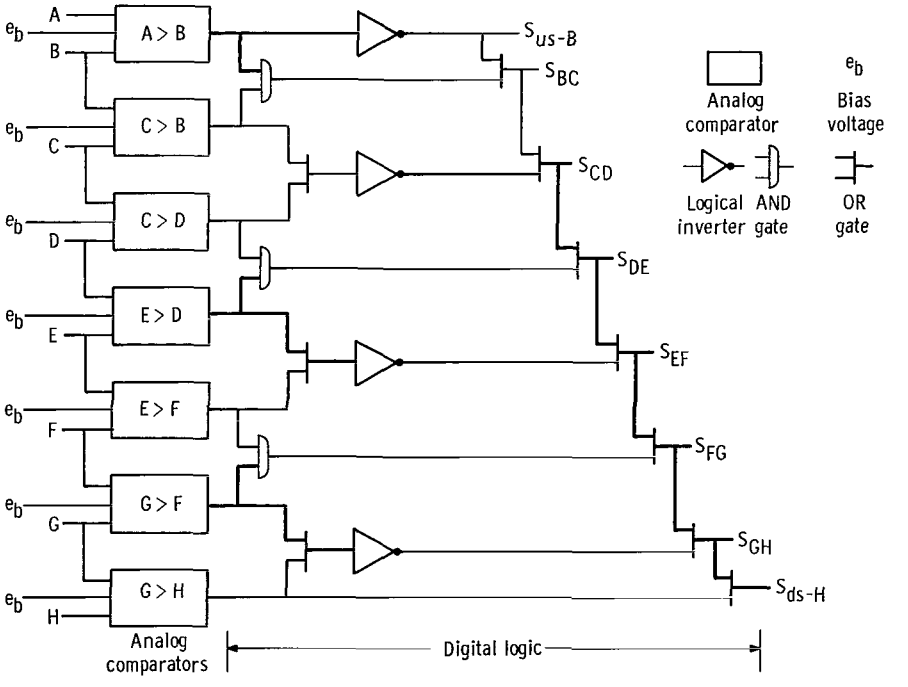

Figure 5. - Actual electronic shock position sensor circuit showing ON-OFF information for case when normal shock is between taps C and D (heavy lines indicate ON outputs).

Biasing of the Supersonic Static Pressure Profile

During wind tunnel test programs, it was occasionally necessary to change the pressure biases due to a change in wind tunnel conditions such as total pressure. In such a case, it was a relatively simple matter to make adjustments experimentally which resulted in correct operation of the sensor. However, the inlet static pressure profile for a given shock position could change rapidly with flight conditions. If the pressure biases are not changed when a disturbance occurs, the shock sensor may not indicate shock position correctly. This might result in an undesirable consequence such as an inlet unstart if the sensor output is being used as the feedback variable for a normal shock control. Changes in the pressure profile could be caused by disturbances such as changes in pressure levels due to altitude changes; aircraft maneuvers; and changes in inlet Mach number due to atmospheric turbulence, variations in atmospheric temperature, or changes in flight Mach number. The effect of such disturbances on the performance of the sensor were not studied during the investigation reported here. However, different disturbances may require different bias adjustments in order for the sensor to operate accurately. It may be necessary to schedule the biases as functions of different flight parameters such as angle of attack and flight Mach number. Investigations should be made to determine how complicated the scheduling would have to be and whether or not it would be practical for flight applications.

EXPERIMENTAL WIND TUNNEL TESTS

Apparatus

Wind tunnel tests of the electronic shock position sensor were conducted in the Lewis 10- by 10-Foot Supersonic Wind Tunnel. The sensor was tested both statically and dynamically in an axisymmetric mixed-compression inlet with 60-percent internal contraction and designed for Mach 2.5. An isometric view of the inlet is presented in figure 6. The inlet capture area was 1760 square centimeters. The results of the tests presented in this report were obtained with the inlet diffuser exit choked.

The inlet had porous bleed regions located on the centerbody and cowl surfaces. These are indicated in figure 6. It should be recalled that the cowl bleeds were believed to have been responsible for the irregular static pressure profiles shown in figure 1. Optimization of the bleed configuration and design and performance details of the inlet are reported in references 2 and 3.

The inlet was equipped with six high-response overboard bypass doors, two of which are shown in figure 6. The bypass doors were located symmetrically around the inlet,

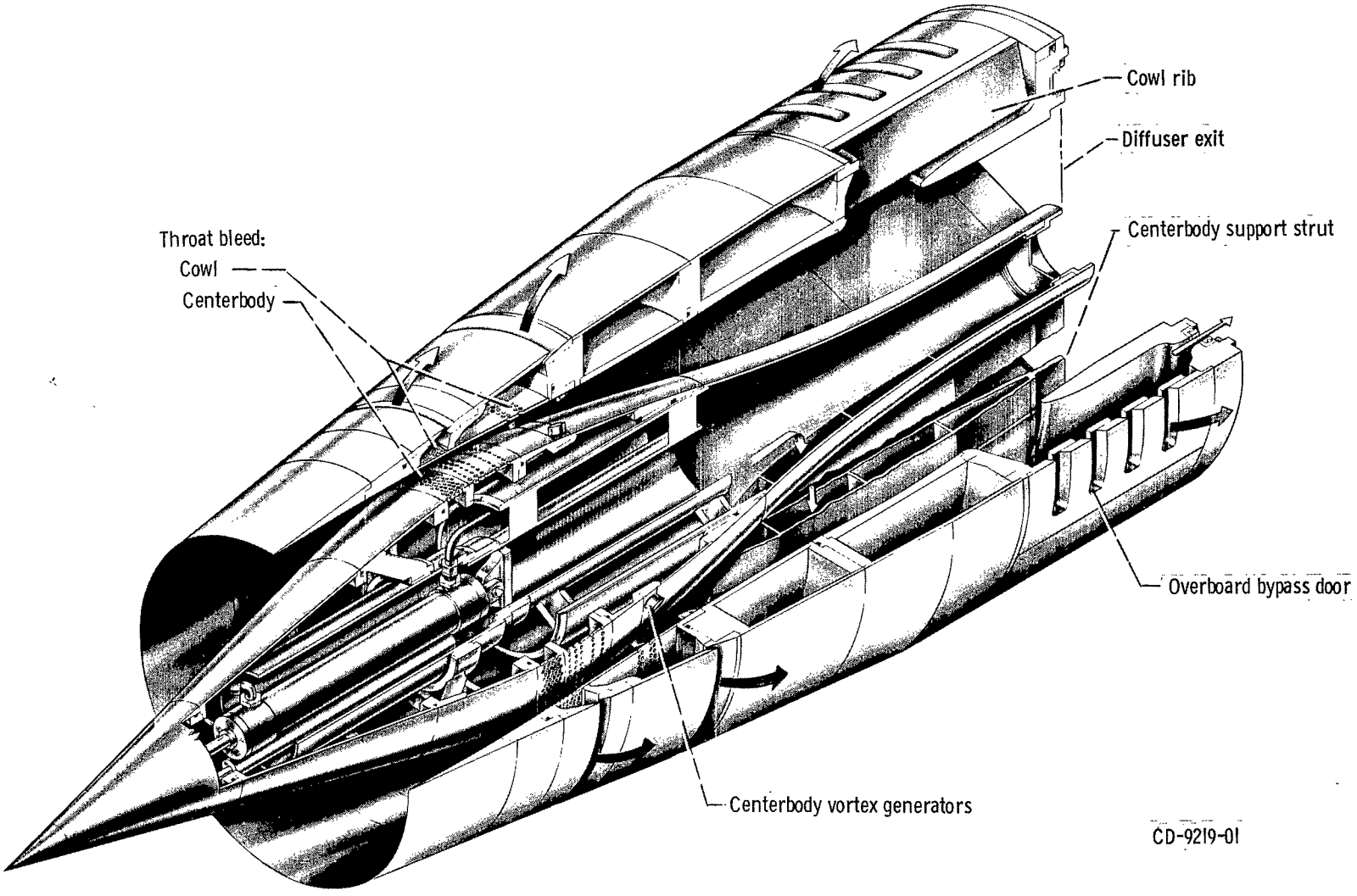

Figure 6. - Isometric view of inlet.

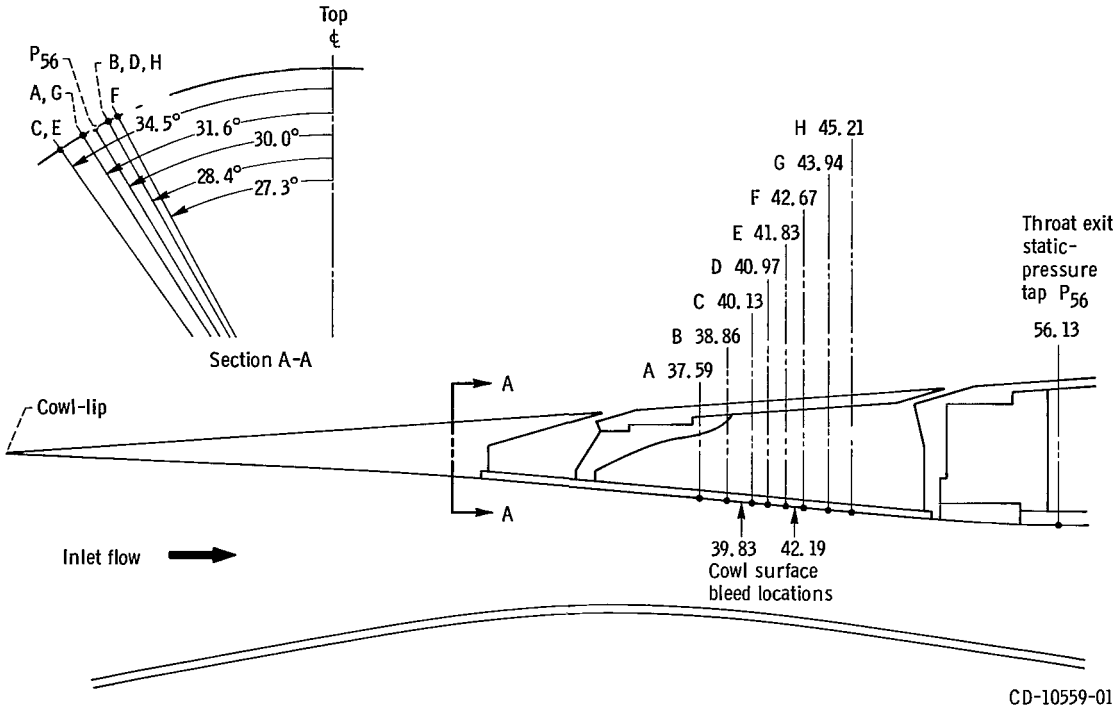

Figure 7. - Inlet throat dynamic instrumentation locations. (Dimensions in centimeters from cowl-lip.)

just upstream of the diffuser exit, and were used to vary shock position. The doors could be controlled individually by means of high response electrohydraulic servomechanisms. The overboard bypass door exits were choked.

The locations of the eight throat static pressure taps (A to H) used to establish the cowl-surface pressure profile are shown in figure 7. The taps were connected to close-coupled electronic pressure transducers. The frequency response of each transducer and its coupled line was flat within 0 to +1 decibel and had a phase lag between 0^{o} and 8^{o} from dc to 180 hertz. The locations of the cowl surface bleeds that were used during the testing are also indicated. Since the inlet throat remained approximately fixed with respect to the centerbody, the pressure taps were located properly with respect to the throat only when the centerbody was at its Mach 2.5 design position. For this reason, tests of the shock sensor were conducted only with the inlet in its Mach 2.5 design configuration. Outputs of the eight pressure transducers were trunked to a ±10 volt desk-top analog computer located in the wind tunnel control room. The computer and a small digital logic panel were used to implement the shock sensor circuit.

Static Tests

Procedure. - The static performance of the sensor was determined by setting the normal shock at positions between each pair of adjacent taps. Actual shock position was determined by noting the most downstream tap that had a pressure level equal to its supersonic value. It was then known that the shock was located between that tap and the adjacent downstream tap. The shock position indicated by the sensor was then compared with the actual shock position.

Static test results. - For static conditions the electronic shock position sensor always indicated the correct shock position (within the spacing of the taps). This was true whether the shock approached the static condition from an upstream or downstream direction.

Dynamic Tests

Procedure. - The response of the electronic shock position sensor to sinusoidal normal shock motion for frequencies out to 65 hertz was measured. The shock motion was produced by oscillating three symmetrically located inlet bypass doors sinusoidally. It was shown in reference 4 that shock travel between A and H is approximately a linear function of bypass door area. An amplitude was chosen such that the shock passed from a location downstream of H to a location upstream of B. By manual adjustment of the input voltage to the bypass door servos, the shock motion amplitude was held approximately constant at all frequencies. The adjustments were necessitated by both bypass door servo dynamics and inlet pneumatic dynamics. The bypass door servo frequency response to a constant amplitude sinusoidal voltage input ΔE is shown in figure 8 and was obtained from reference 5. Unless otherwise noted, all amplitude ratio data shown in this report have been divided by their respective 1 hertz value. Figure 9 shows the frequency response of shock position amplitude Δx_a to a sinusoidal bypass door disturbance ΔA_{by} and was taken from reference 4. The 1 hertz bypass door area zero-to-peak amplitude was about the same for the tests of figures 8 and 9 and gave about the same peak-to-peak shock position amplitude that was used for the dynamic tests. Because of physical limitations of bypass door hardware, it was possible to maintain the constant shock position amplitude out to a frequency of only 65 hertz.

Dynamic test results. - Figures 10(a) to (f) show results of tests where the inlet was subjected to sinusoidal bypass area variations at frequencies of 1, 11, 20, 35, 53, and 65 hertz, respectively. They are oscillograph traces of the sensor's stepwise continuous output signal and the eight throat static pressure transducer signals. The arrows indicate the direction of increasing pressure and the base of each arrow is at the super-

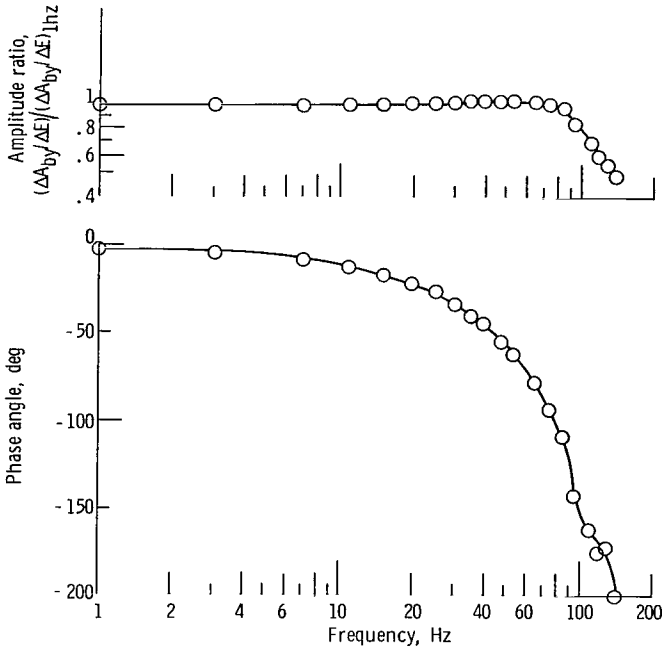

Figure 8. - Bypass door frequency response.

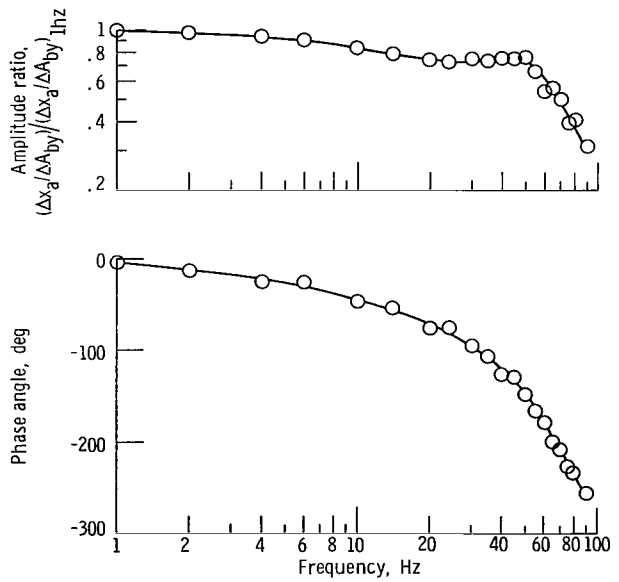

Figure 9. - Dynamic response of shock position to symmetrical internal downstream disturbance, diffuser exit choked.

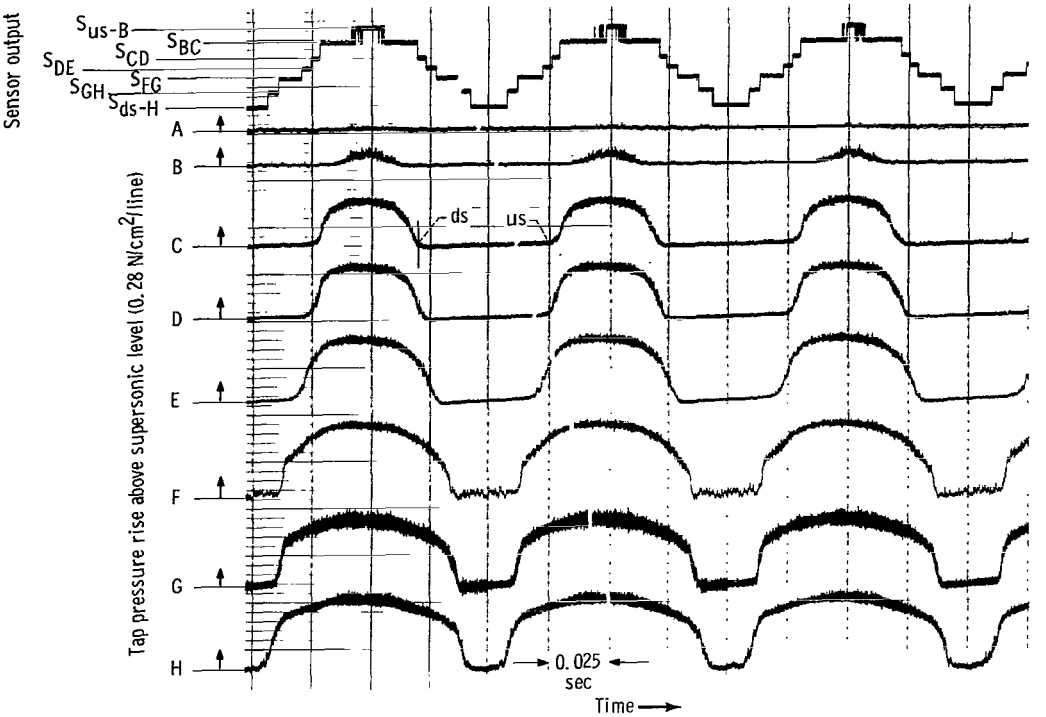

(a) Frequency, 1 hertz.

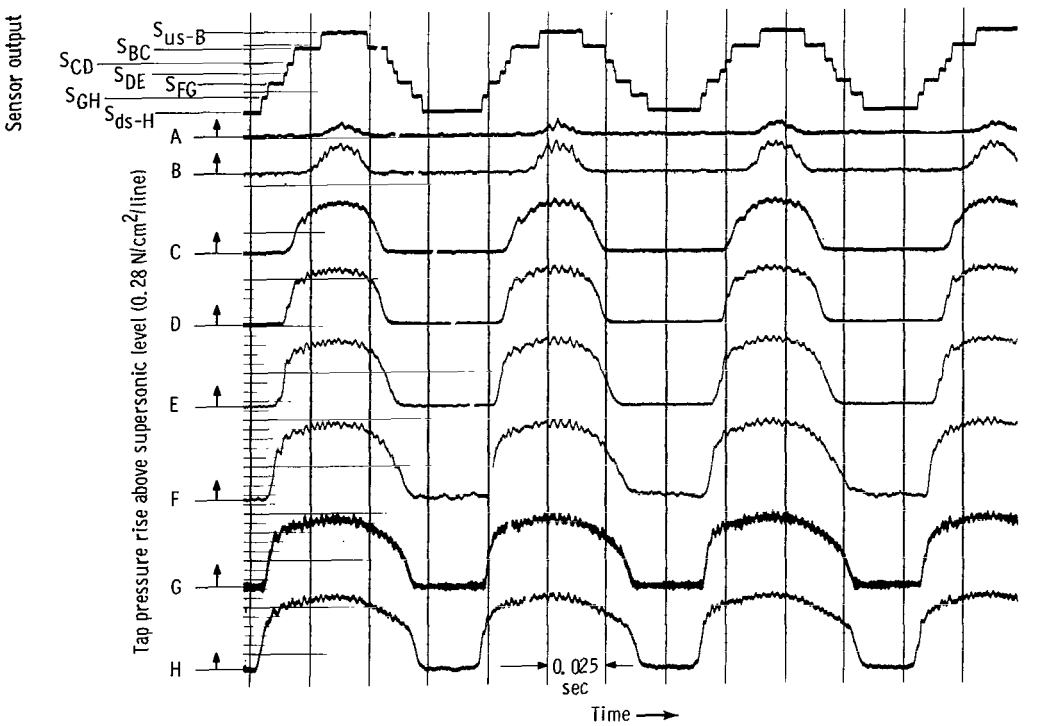

(b) Frequency, 11 hertz.

Figure 10. - Shock sensor time response to sinusoidal normal shock motions at frequencies from 1 to 65 hertz. (All pressure trace supersonic levels are approximately the same as those of figure 1.)

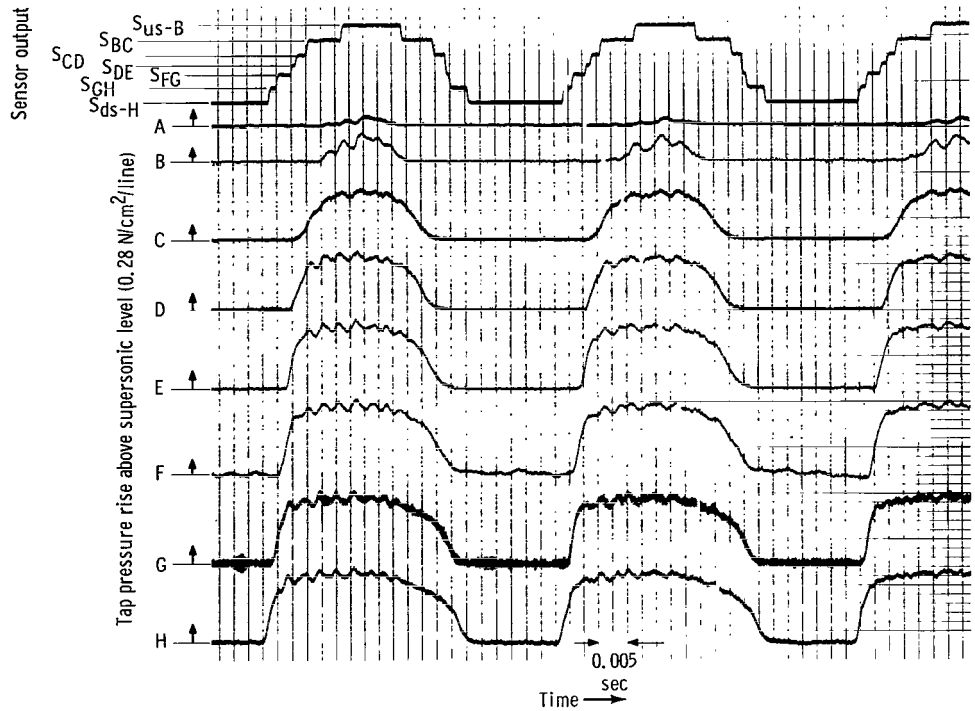

(c) Frequency, 20 hertz.

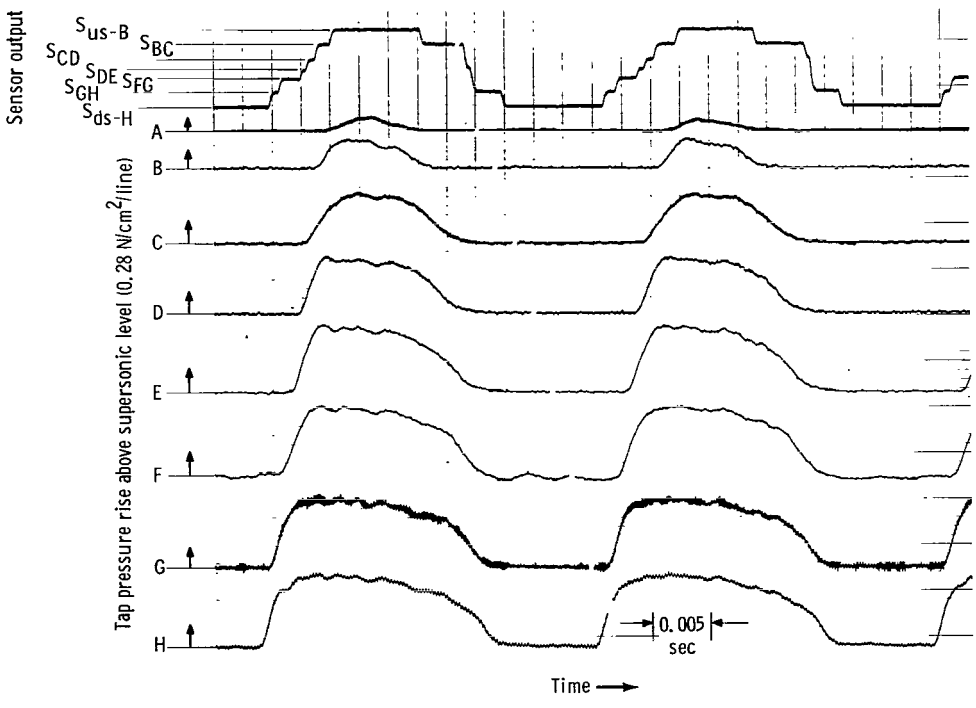

(d) Frequency, 35 hertz.

Figure 10. - Continued.

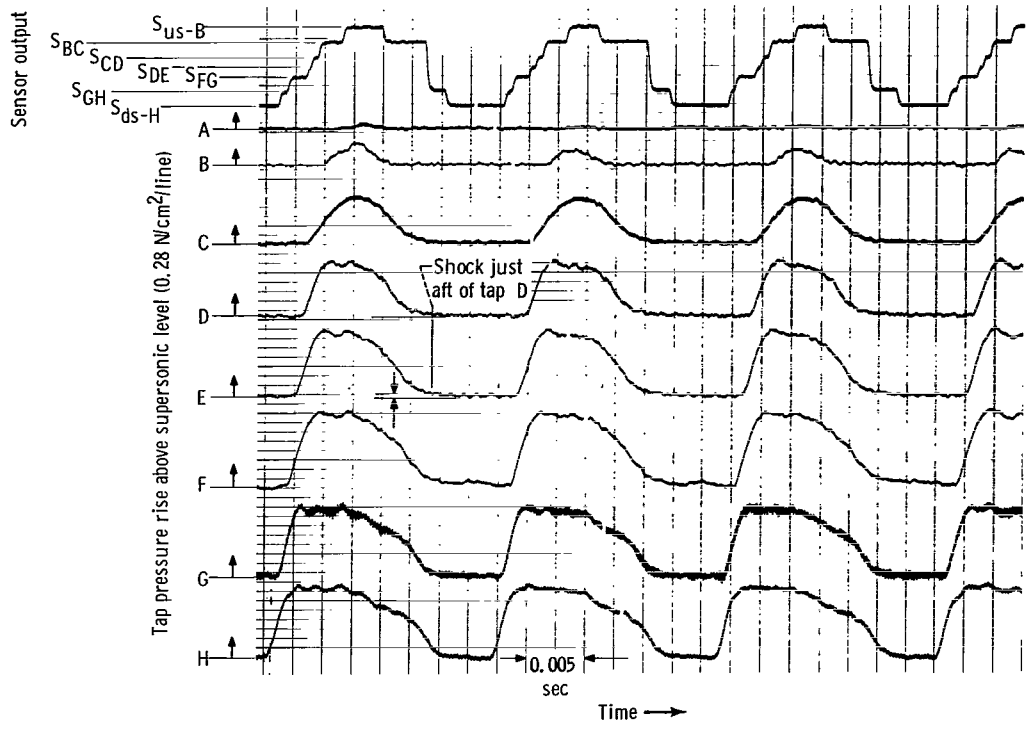

(e) Frequency, 53 hertz.

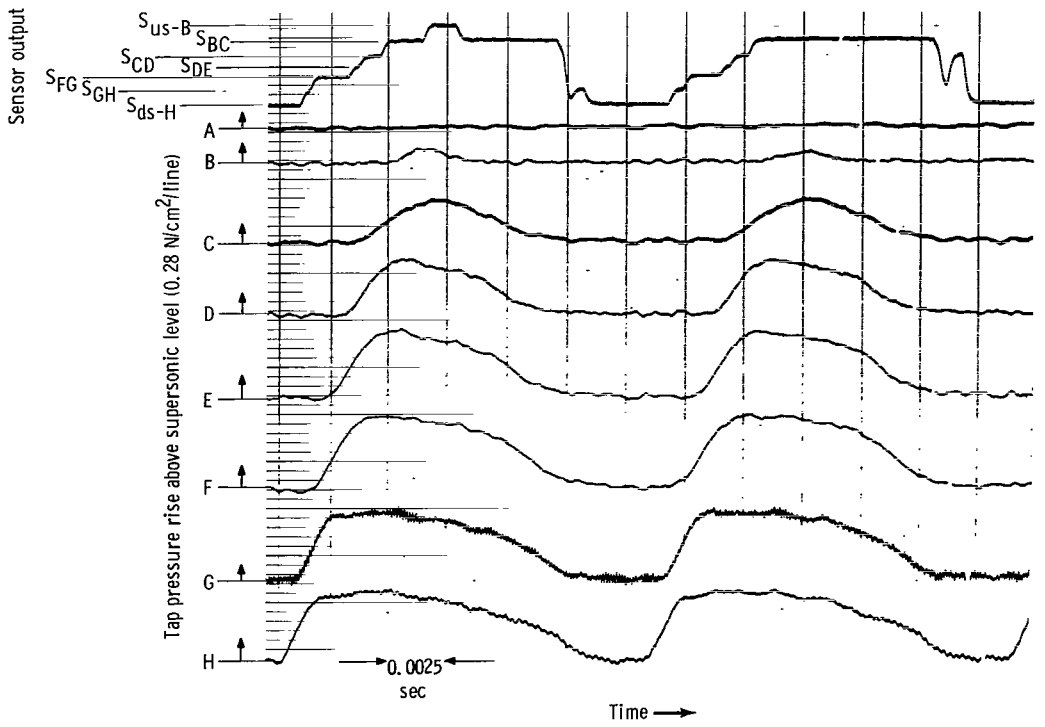

(f) Frequency, 65 hertz.

Figure 10. - Concluded.

sonic pressure level of the trace. The approximate magnitude of the supersonic pressure level at each tap can be determined from the supersonic pressure distribution shown in figure 1. The pressure transducer outputs were conditioned by high pass filters before being recorded. The filters had zero output for dc signals and a corner frequency of 0.5 radians per second (0.08 Hz). In figures 10, the S_{EF} output level is not included in the sensor output signal trace. It was discovered after completion of the test program that the S_{EF} output was not summed into the sensor output signal.

Methods of analysis. - In order to analyze the shock sensor dynamic test results, it was necessary to establish a criterion for determining actual shock position. The best available aid for determining actual shock position was the pressure traces of the eight throat static pressure taps. Actual shock position was assumed to be at a pressure tap when the trace changed from its supersonic level to a subsonic level or vice versa. The portions of a tap pressure trace, which are of relatively constant value, indicate that the tap is in a supersonic flow region (i.e., the shock is aft of the tap). For example, two points at which the shock is just passing tap C in the downstream and upstream directions during the 1-hertz test of figure 10(a) are denoted by ds and us, respectively. The normal shock is downstream of tap C for the portion of the trace between ds and us.

Discrete shock position information can also be obtained from the shock sensor output signal by observing when the sensor switches from one level to another. For example, when the shock is moving in the downstream direction the sensor should switch from S_{BC} to S_{CD} just after the shock passes tap C.

Since the pressure taps and the shock sensor output do not provide continuous measures of shock motion, it is difficult to determine amplitude and phase information that is usually obtained from frequency response tests. However, since the shock motion is approximately sinusoidal, average continuous shock paths can be obtained by fitting both the pressure trace and the sensor discrete position data with sine waves by the method of least squares. This method of analysis (suggested in ref. 6) is illustrated graphically in figure 11 using the 11-hertz test data of figure 10(b). A digital computer program was used to fit several cycles of discrete position data with a sine wave of the form $\Delta x \sin(\omega t + \varphi)$ by the method of least squares where Δx is the zero to peak amplitude of the shock motion, ω is the frequency of shock motion (assumed to be the same as the disturbance frequency), and φ is the phase angle with respect to the time reference. The sine waves thus provide a means for calculating an overall phase shift, $\varphi_s - \varphi_a$, between actual shock position and the sensor's stepwise continuous output signal. The subscripts a and s refer to actual shock motion as determined by curve fitting the tap crossings and the sensor output, respectively. Measures of actual shock amplitude Δx_a and shock amplitude as indicated by the shock sensor Δx_s are also available for comparison.

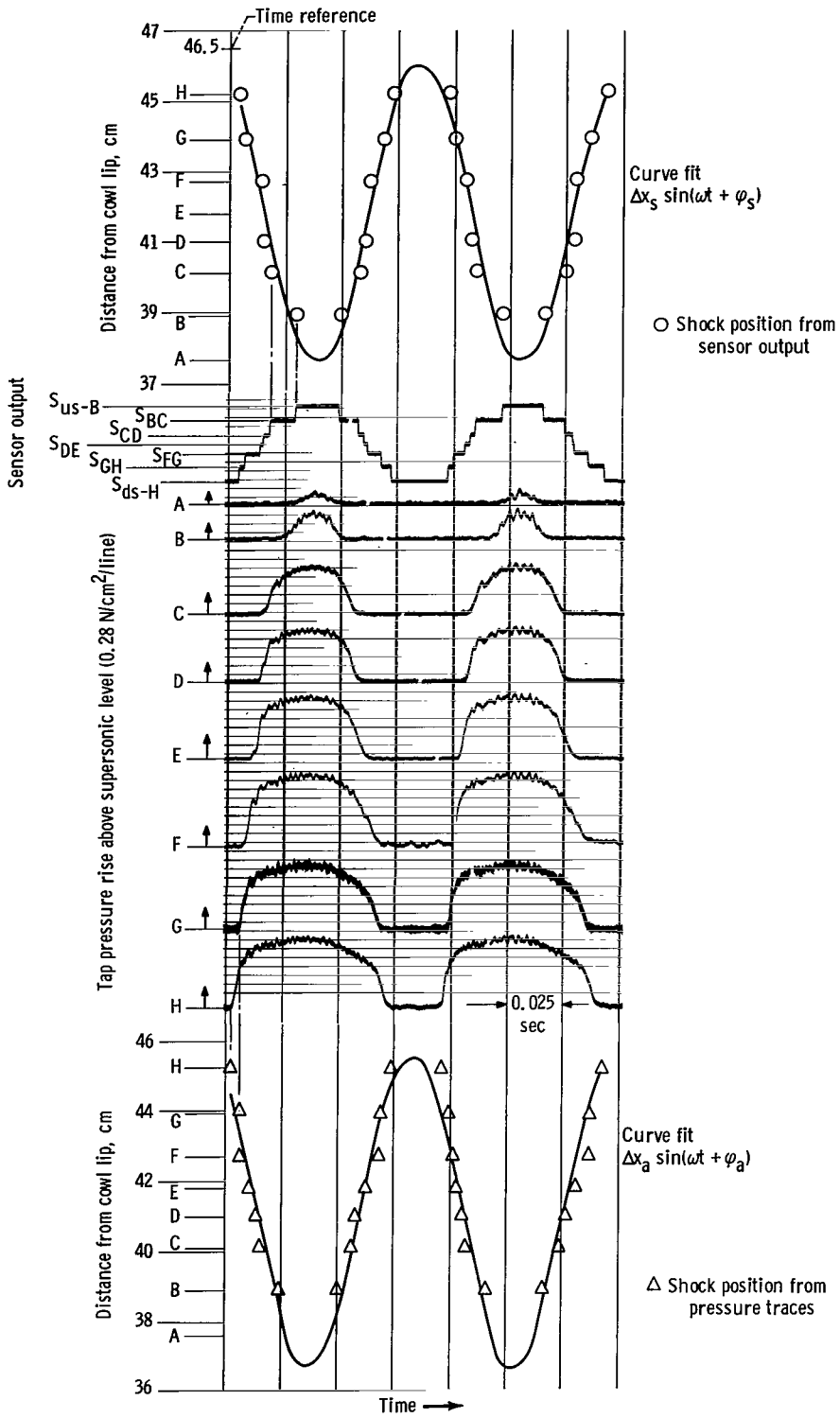

Figure 11. - Graphic illustration of least squares curve fit technique used to determine shock motion from pressure traces and shock sensor output signal. Frequency, 11 hertz.

A more detailed method of analysis would be to compare individual pressure tap crossings by the shock with tap crossings as indicated by the sensor. Such an analysis provides an insight into why the sensor failed to indicate shock position perfectly.

Evaluation of dynamic test results. -

Amplitude and phase analysis: The amplitude and phase results are shown in figure 12 where amplitude ratio $\Delta x_s/\Delta x_a$ (not divided by the 1-Hz value) and phase shift $\varphi_s - \varphi_a$ are plotted as functions of test frequency in hertz. The results show that the shock sensor measures shock zero to peak amplitude within ±10 percent of the actual shock amplitude over the frequency range from 1 to 65 hertz. The zero-to-peak shock position amplitude was maintained between 3.8 and 5.0 centimeters during the dynamic tests. Thus, for sinusoidal shock motion the maximum error in shock amplitude indicated by the sensor was 0.5 centimeter which is less than the minimum tap spacing of 0.84 centimeter.

Figure 12 also shows that the shock sensor lags actual shock motion by 7° or less for frequencies out to 35 hertz and increases to a lag of about 18° at 65 hertz. The digital logic elements had switching times of 2 microseconds or less and therefore did not contribute to the sensor's lagging phase shift. However, as will be shown later, the analog comparators may have contributed to the lag. In any event, the results indicate that the shock sensor followed sinusoidal shock motions very well.

The shock sensor's indication of shock motion can be contrasted to a single pressure downstream of the normal shock such as the throat exit static pressure P_{56} of figure 7. Figure 13 shows amplitude ratio and phase characteristics of P_{56} as compared with actual shock amplitude and phase. The data were reported in reference 4. The data show that the P_{56} amplitude ratio is in error by as much as 20 percent which is not significantly greater than the shock sensor's amplitude error. However, P_{56} exhibits a phase shift which increases from 0° at 1 hertz to 85° at 65 hertz. Thus, it appears that, on the basis of phase shift, the shock sensor provides a better indication

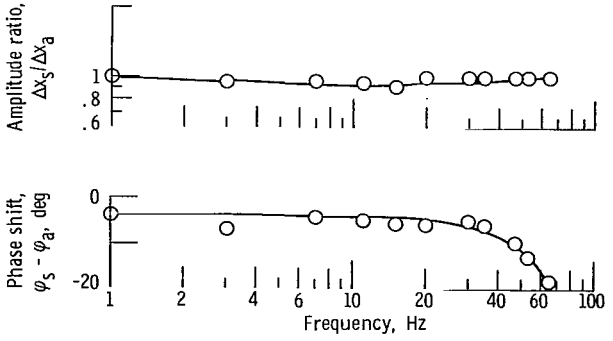

Figure 12. - Frequency response of shock sensor output to sinusoidal shock motion. Amplitude and phase determined by method of least squares.

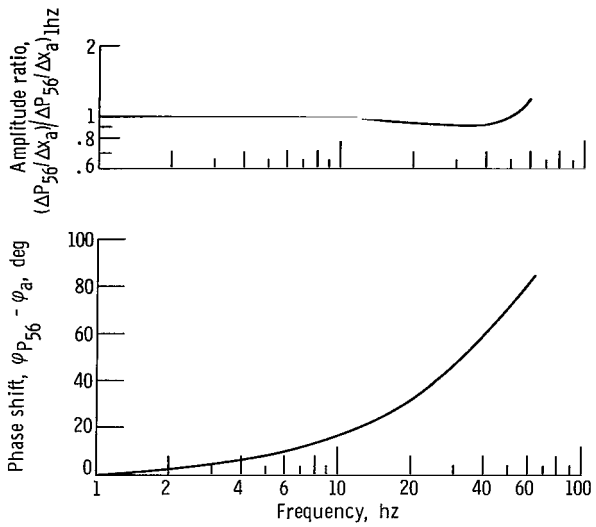

Figure 13. - Frequency response of throat exit static pressure P_{56} to sinusoidal shock motion, diffuser exit choked.

of shock motion than does the throat exit static pressure when the inlet is subjected to downstream disturbances.

Analysis of individual pressure tap crossings: The previous section shows that on the average the shock sensor slightly lags actual shock motion. This, of course, means that on the average the shock sensor output does not switch to a new level at exactly the same instant that the shock passes a tap. The sensor does not switch at exactly the right instant because the normal shock in the inlet is not ideal (i. e., the pressure rise across the normal shock does not have an infinite slope). In addition, a tap pressure will be influenced before the shock is actually at the tap because of shock-boundary layer interactions. These nonideal characteristics make it difficult to define actual shock position. An example of the nonideal nature of the shock is illustrated in figure 1 by means of the pressure profile denoted by the symbol D. Since the pressure at tap C is higher than the supersonic pressure level of tap C, actual shock position would be defined as between taps B and C. The shock sensor, on the other hand, would determine the shock position to be between taps C and D because the most forward minimum in the pressure profile occurs at tap C.

Since the shock moved over taps B to H for all tests shown in figures 10, the sensor output signal should exhibit seven different levels since the S_{EF} level was omitted. The sensor output did have seven different levels for the 1- and 11-hertz tests of figures 10(a) and (b), respectively. However, the S_{DE} level does not appear in the sensor output signal for downstream shock excursions during the 20-hertz test of figure 10(c). As frequency was increased, additional levels were omitted from the sensor output signal

during downstream excursions of the shock. Table I shows which sensor output levels were omitted during downstream and upstream excursions of the shock for the test frequencies of figures 10.

TABLE I. - TAP CROSSINGS BY NORMAL SHOCK AS INDICATED BY SHOCK SENSOR OUTPUT DURING DOWNSTREAM AND UPSTREAM SHOCK EXCURSIONS

Frequency, Hz	Shock moving downstream						Shock moving upstream					
	S_{BC}	S_{CD}	S_{DE}	S_{FG}	S_{GH}	S_{ds-H}	S_{GH}	S_{FG}	S_{DE}	S_{CD}	S_{BC}	S_{us-B}
1	x	x	x	x	x	x	x	x	x	x	x	x
11	x	x	x	x	x	x	x	x	x	x	x	x
20	x	x	0	x	x	x	x	x	x	x	x	x
35	x	s	s	0	x	x	x	x	x	x	x	x
53	x	0	0	0	x	x	x	x	s	x	x	x
65	x	s	0	0	s	x	x	x	x	x	x	s

x denotes shock was always indicated; 0 was never indicated; s was sometimes indicated.

The following facts are observed from table I: (1) with two minor exceptions, the sensor never omitted a level during upstream shock excursions; (2) during downstream excursions at frequencies of 20 hertz or above, the sensor omitted levels for tap crossings closest to the shock operating point (center of shock motion). The omission of levels from the sensor output signal resulted from a combination of inherent shock dynamics and the analog comparators used in the shock sensor circuit.

Different inlet pressure profiles are generated by upstream and downstream shock excursions. This can be observed by noting that the subsonic portion of the pressure traces are not exactly symmetrical. The asymmetry of the traces is more evident at higher frequencies. The 53-hertz test of figure 10(e), for instance, shows that the pressure rise across the shock is much steeper for the upstream shock excursion than it is for the downstream shock excursion. This agrees with the theory of moving normal shocks. It can be shown that, for adiabatic conditions and thermally perfect air, the static pressure rise across a normal shock depends on the Mach number of the airflow just ahead of the shock according to the relation

$$\frac{P_2}{P_1} = \frac{(7M_{1R}^2 - 1)}{6}$$

where the subscripts 1 and 2 refer to stations just upstream and downstream of the shock, respectively, and the Mach number M_{1R} is measured relative to the normal shock. The relative Mach number can be expressed as

$$M_{1R} = \frac{M_1 - \dot{x}_a}{a_1}$$

where M_1 is the Mach number ahead of the shock measured from a fixed inlet station, $\dot{x}_a$ is the normal shock velocity (assumed positive in the downstream direction), and a_1 is the speed of sound ahead of the shock. M_{1R} would thus be higher when the shock is traveling upstream.

It is concluded then that the pressure rise due to the shock between two adjacent taps is generally less for downstream shock excursions than for upstream shock excursions. The switching times of the analog comparators (from one voltage level to the other) were significantly affected by the magnitude of the input voltage which was proportional to the pressure difference between the pressures being compared. A detailed sketch of a comparator and its switching time as a function of step input voltages of different magnitudes are shown in figure 14. The shock sensor circuit used 100 millivolts as the equivalent of 0.69 newtons per square centimeter. It is believed that the pressure differentials between

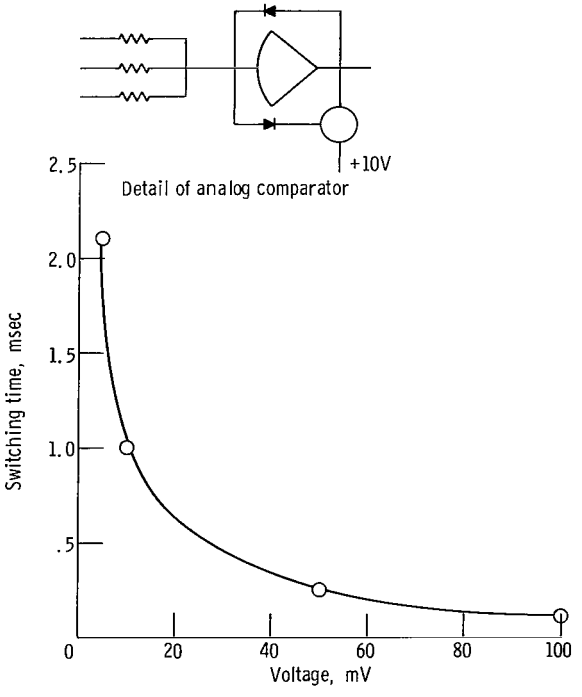

Figure 14. - Comparator switching time as function of step input voltage of either polarity.

taps during downstream shock excursions were occasionally small enough to result in comparator switching times that were longer than the time it took the shock to move between the taps. In such cases, the corresponding output level would be omitted from the sensor's stepwise proportional signal. The validity of this theory is illustrated by considering the 53-hertz test of figure 10(e) and specifically the comparison of pressures at taps E and D. The maximum pressure difference between any two adjacent taps occurs when the shock is just aft of the most upstream of the two taps. The maximum pressure difference between taps D and E during a downstream shock excursion is calculated as follows:

(1) The biased supersonic values of taps D and E are first found from figure 2 to be 3.52 and 3.45 newtons per square centimeter, respectively.

(2) When the shock is moving downstream and is just aft of tap D, the pressure at tap D is equal to its supersonic value and the pressure at tap E is approximately one-third of a line (or 0.09 N/cm^2) above its supersonic value. Thus, the pressures at taps D and E were approximately 3.52 and 3.54 newtons per square centimeter, respectively, or a difference of 0.02 newtons per square centimeter.

The voltage equivalent to the maximum difference in pressure between taps D and E for the downstream excursion is then calculated to be approximately 3 millivolts. The corresponding switching time of the comparator is found from figure 14 to be approximately 2 milliseconds. Since taps D and E are near the shock operating point, the shock velocity would have approximately the maximum value $\omega\Delta x_a$ in the vicinity of taps D and E. The shock zero-to-peak amplitude for the 53-hertz test was found by the curve fitting technique to be 4.4 centimeters giving a maximum shock velocity of 1470 centimeters per second. The shock took approximately 0.6 millisecond to pass between taps D and E which were spaced 0.86 centimeter apart. Therefore, the comparator switching time was more than three times as long as the time it took the shock to move between taps D and E in the downstream direction. This accounts for the S_{DE} output being omitted from the sensor output signal during downstream shock excursion of the 53-hertz test. It is believed that this phenomenon was also responsible for the other output levels being omitted from the sensor's output signal. The comparator switching time therefore accounts in part for the lagging phase shift of the sensor with respect to actual shock motion. Figure 14 indicates that the omission of levels from the sensor output could be avoided by using higher pressure signal gains or by using faster comparators.

APPLICATIONS

Determination of Shock Position Frequency Response

Shock motion can be estimated to a fair degree of accuracy by fitting the shock sensor stepwise continuous output signal with a sine wave by the method of least squares. However, that method is quite tedious and time-consuming. An easier method to determine phase and amplitude from the sensor output signal is to use one of the commercially available electronic frequency response analyzers. Such analyzers may have a sinusoidal output signal which can be used to drive the disturbance device. By various correlation techniques, the analyzers determine the feedback signal amplitude in volts and phase angle (with respect to a driving signal). Such a device was used to analyze the sensor output signal. In figure 15 the measure of shock amplitude and phase that were obtained with the frequency response analyzer are denoted as indicated shock amplitude Δx_i and phase angle φ_i. Values of amplitude ratio $\Delta x_i/\Delta x_a$ and phase shift $\varphi_i - \varphi_a$ are plotted as a function of the test frequency. Figure 15 shows the indicated amplitude to be within 10 percent of the actual amplitude over the range of test frequencies shown except at 30 hertz where there was a 15-percent error. The sensor phase lag is shown to be 5^o or less out to 35 hertz and then increases to approximately 25^o at 65 hertz. Thus the amplitude and phase data obtained with the frequency response analyzer are in good agreement with the corresponding data of figure 12 obtained by means of the curve fitting technique.

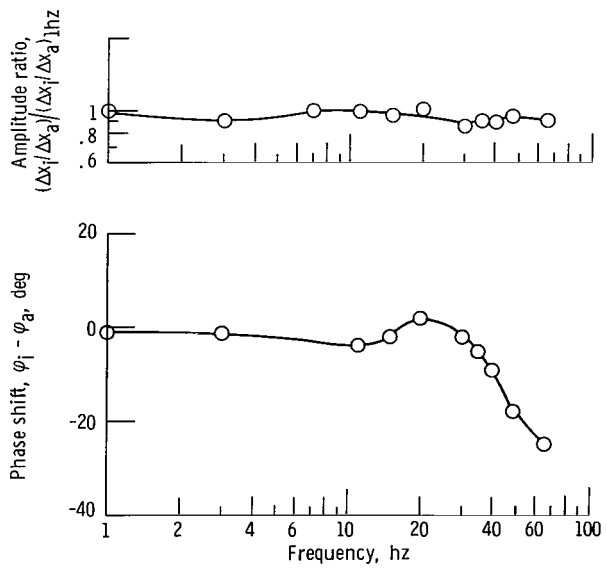

Figure 15. - Frequency response of shock sensor output (as measured by a frequency response analyzer) to sinusoidal shock motion.

The difference is due to the analyzer characteristics. Besides being faster, the frequency response analyzer also offers the advantage of being able to obtain shock position frequency responses during a test.

Either the curve fitting technique or the frequency response analyzer can be used to evaluate open and closed loop frequency response tests of shock motion to airflow disturbances. An example of shock position control performance is illustrated in figure 16 which shows a closed loop shock amplitude frequency response. The control used P_{56} as the feedback variable. The frequency response was determined from the shock sensor's stepwise continuous output signal by means of a frequency response analyzer. The ratio of indicated shock amplitude Δx_i to the amplitude of the sinusoidal bypass disturbance ΔA_{by} is plotted against frequency. In this case, all $\Delta x_i/\Delta A_{by}$ data were normalized by the 1-hertz open loop value of the ratio. Thus the normal shock control results in a 90 percent reduction of shock amplitude at 1 hertz.

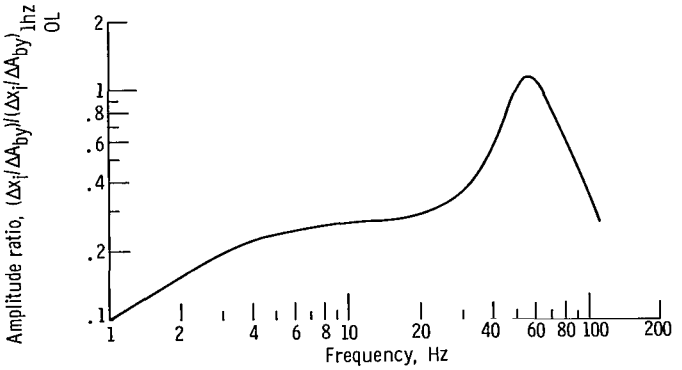

Figure 16. - Example of normal shock control performance as determined from shock sensor stepwise continuous output by means of frequency response analyzer.

Use of Sensor Output as Feedback Signal

It was already demonstrated in figure 12 that the sensor stepwise continuous output signal provides an excellent indication of shock position. It would seem appropriate to use this signal as a terminal shock control feedback variable.

A proportional type normal shock control was tested using the shock sensor output signal as the feedback variable. The same control was also tested using the throat exit static P_{56} as the feedback variable but with a slightly higher gain. The shock position amplitude frequency responses of the inlet with the two controls were determined by subjecting the inlet to sinusoidal bypass door disturbances and the results are shown in figure 17. As in figure 16, the amplitudes Δx_i were determined from the shock sensor

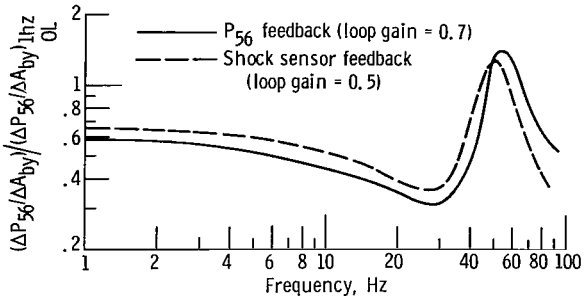

Figure 17. - Comparison of frequency responses of shock position to sinusoidal bypass door disturbances with proportional normal shock control using either shock sensor output or throat exit static pressure P_{56} feedback.

output by a frequency response analyzer. The ordinate is the ratio of Δx_i to the bypass door amplitude ΔA_{by} divided by the 1-hertz open loop value of $\Delta x_i/\Delta A_{by}$. The two responses indicate that P_{56} and shock position feedback give approximately the same results for proportional control. This suggests that the sensor output signal would also be suitable as a feedback variable for more complex controllers.

Shock Sensor Output Used for Visual Aid

The shock sensor provided a visual aid for determining shock position in the control room. This was done by connecting each output level to lights on the digital logic panel which represented the eight static pressure taps. The shock position was visually determined to be between the most upstream light that was on and the adjacent downstream light (except when all eight lights were on indicating the shock was either between taps A and B or upstream of A). The light indication of shock position proved to be extremely useful for setting up peak-to-peak shock position amplitudes for dynamic inlet tests as well as for positioning the shock during steady-state testing.

SUMMARY OF RESULTS

This report presents the design features and experimental performance of a digital electronic normal shock position sensor for an axisymmetric mixed-compression inlet. The sensor determines shock position by sensing the most forward minimum in the cowl surface static pressure profile. It is demonstrated that this criterion for determining shock position is feasible. The sensor generates an electronic stepwise continuous signal which is proportional to shock position. Results of static tests demonstrate that the

sensor indicated shock position correctly within the spacing of the throat static pressure taps. The dynamic response of the sensor for sinusoidal shock motion is shown to agree within 10 percent of actual shock amplitude. However, the sensor output exhibits a lagging phase shift of from 4^{o} to 18^{o} with respect to actual shock motion, over the test frequency range of 1 to 65 hertz. The dynamic test results also show that some levels are omitted from the sensor stepwise continuous output signal during downstream shock excursions at frequencies of 20 hertz and higher. The omission of levels is due to the slow response of the analog comparator circuits used and the lower pressure rise across the shock when it is moving in the downstream direction. Using higher pressure signal gains or faster comparators should make it possible to eliminate the problem. For the constant conditions in the wind tunnel, the overall performance of the sensor was very good. The sensor provided a more direct indication of shock position during dynamic tests than did a throat exit static pressure.

The requirement of electronic biasing, to eliminate false indications of shock position, could create problems in a flight application of the sensor. Such biases might have to be scheduled as functions of several variables such as flight Mach number and angle of attack. It is recommended that further work be performed to find ways to minimize or eliminate the need for biasing. This might be accomplished by adding logic to the present system or by using a different shock position criterion.

The shock sensor has practical applications during static and dynamic wind tunnel tests of inlets. The sensor is a valuable aid for determining both open and closed loop frequency responses of the inlet's normal shock to sinusoidal disturbances. A light indicator of shock position proved to be useful for setting peak-to-peak shock amplitudes for dynamic tests and for shock positioning during steady-state tests.

Lewis Research Center,
National Aeronautics and Space Administration,
Cleveland, Ohio, August 25, 1969,
720-03.

REFERENCES

1. Griffin, William S.: Design and Performance of a Flueric Shock Position Sensor for a Mixed-Compression Supersonic Inlet. NASA TM X-1733, 1969.

2. Cubbison, Robert W.; Meleason, Edward T.; and Johnson, David F.: Effect of Porous Bleed in a High-Performance, Axisymmetric, Mixed-Compression Inlet at Mach 2.50. NASA TM X-1692, 1968.

3. Cubbison, Robert W.; Meleason, Edward T.; and Johnson, David F.: Performance Characteristics from Mach 2.58 to 1.98 of an Axisymmetric, Mixed-Compression Inlet System with 60-Percent Internal Contraction. NASA TM X-1739, 1969.

4. Wasserbauer, Joseph F.: Dynamic Response of a Mach 2.5 Axisymmetric Inlet with Engine or Cold Pipe and Utilizing 60 Percent Supersonic Internal Area Contraction. NASA TN D-5338, 1969.

5. Crosby, Michael J.; Neiner, George H.; and Cole, Gary L.: Restart and High Response Terminal Shock Control for an Axisymmetric Mixed-Compression Inlet with 60-Percent Internal Contraction. NASA TM X-1792, 1969.

6. Wasserbauer, Joseph F.; and Whipple, Daniel L.: Experimental Investigation of the Dynamic Response of a Supersonic Inlet to External and Internal Disturbances. NASA TM X-1648, 1968.

NASA-Langley, 1969 —— 14 E-5223

NATIONAL AERONAUTICS AND SPACE ADMINISTRATION
WASHINGTON, D. C. 20546

OFFICIAL BUSINESS

FIRST CLASS MAIL

POSTAGE AND FEES PAID
NATIONAL AERONAUTICS AND
SPACE ADMINISTRATION

POSTMASTER: If Undeliverable (Section 158 Postal Manual) Do Not Return

"The aeronautical and space activities of the United States shall be conducted so as to contribute . . . to the expansion of human knowledge of phenomena in the atmosphere and space. The Administration shall provide for the widest practicable and appropriate dissemination of information concerning its activities and the results thereof."

—NATIONAL AERONAUTICS AND SPACE ACT OF 1958

NASA SCIENTIFIC AND TECHNICAL PUBLICATIONS

TECHNICAL REPORTS: Scientific and technical information considered important, complete, and a lasting contribution to existing knowledge.

TECHNICAL NOTES: Information less broad in scope but nevertheless of importance as a contribution to existing knowledge.

TECHNICAL MEMORANDUMS: Information receiving limited distribution because of preliminary data, security classification, or other reasons.

CONTRACTOR REPORTS: Scientific and technical information generated under a NASA contract or grant and considered an important contribution to existing knowledge.

TECHNICAL TRANSLATIONS: Information published in a foreign language considered to merit NASA distribution in English.

SPECIAL PUBLICATIONS: Information derived from or of value to NASA activities. Publications include conference proceedings, monographs, data compilations, handbooks, sourcebooks, and special bibliographies.

TECHNOLOGY UTILIZATION PUBLICATIONS: Information on technology used by NASA that may be of particular interest in commercial and other non-aerospace applications. Publications include Tech Briefs, Technology Utilization Reports and Notes, and Technology Surveys.

Details on the availability of these publications may be obtained from:

SCIENTIFIC AND TECHNICAL INFORMATION DIVISION

NATIONAL AERONAUTICS AND SPACE ADMINISTRATION

Washington, D.C. 20546